# Size-Dependent Orientation Growth of Large-Area Ordered Ni Nanowire Arrays

**Xue Wei Wang, Guang Tao Fei,* Xi Jin Xu, Zhen Jin, and Li De Zhang**

*Key Laboratory of Materials Physics, Institute of Solid State Physics, Hefei Institutes of Physical Science, Chinese Academy of Sciences, P.O. Box 1129, Hefei 230031, P. R. China*

*Received: July 3, 2005; In Final Form: November 1, 2005*

Large-area ordered Ni nanowire arrays with different diameters have been fabricated by the direct current electrodeposition into the holes of porous anodic alumina membrane. The crystal structure and micrograph of nanowire arrays are characterized by X-ray diffraction, field-emission scanning electron microscopy and high-resolution transmission electron microscopy. The results indicate that the growth orientation of Ni nanowires turns from [110] to [111] direction with increasing diameters of nanowires. The mechanism of the growth was discussed in terms of interface energy minimum principle. The size-dependent orientation of Ni nanowire arrays has the important significance for the design and control of nanostructures.

## Introduction

Over the past decade nanostructured materials have attracted considerable research interesting for their potential utilization in nanoelectric devices,[1] high-density magnetic memories,[2] high-performance catalysts,[3] and biomaterial separation membranes[4] and so on. Moreover, the physical properties of nanomaterials have been studied in detail.[5−7] Many physical properties of nanomaterials are different from those of bulk materials with the same chemical components, and one important result is that the physical properties will change with reducing dimension of nanomaterials.[8−11] It is well-known that many physical properties of materials are strongly dependent on the orientation, which leads us to associate the growth orientation with the dimension of nanomaterials. However, little attention is focused on the relation between the orientation and the dimension, especially for nanowires. In general, most people think that there is no relation between the growth orientation and the diameter of nanowires.[12−14] Recently, Lieber's group[15] prepared single-crystal Si nanowires with different diameters by using the chemical vapor deposition (CVD) method and discussed the relation between growth orientation and diameter of Si nanowires, which indicates that there is the relation between growth orientation and diameter of nanowires. Therefore, the relation between growth orientation and diameter of nanowires needs to be further researched.

As we know, Ni is an important material that has been found to have many applications in the magnetic memories. The orientation of Ni nanomaterials is of considerable importance because it directly relates to the direction of the easy magnetic axis, the application strong anisotropy, as well as magnetic isotropy. The growth orientation of Ni nanomaterials has been investigated in the past decade. Abel et al.[16] prepared Ni nanocrystals with perfect [110] and [100] orientation by adjusting experiment parameters. Rahman et al.[17] and Pan et al.[18] discussed the dependence of growth orientation of Ni nanowires on the electrodeposition parameters. They found that the pH value of electrolyte and deposition potential have no effect on the orientation of Ni nanowires, but the temperature of electrolyte has a significant effect on the orientation of nanowires. To our best knowledge, no research has paid attention to the relation between growth orientation and diameter of Ni nanowires. In this paper, we take Ni nanowires as an example to study the relation between growth orientation and diameter, and discuss the mechanism of size-induced orientation transition.

**TABLE 1: Anodizing Conditions Used for Preparing Well-Ordered Holes on Aluminum in Acid Electrolytes**

| electrolyte | concentration (M) | cell voltage (V) | temperature (°C) |
|---|---|---|---|
| $H_2SO_4$ | 0.3 | 24 | 2 |
| $H_2C_2O_4$ | 0.3 | 40 | 5 |
| $H_3PO_4$ | 0.1 | 165 | 3 |

## Experimental Section

The porous anodic alumina membrane (PAAM) templates were prepared by a two-step anodization process as described previously.[19,20] Prior to anodizing, high-purity aluminum foils (99.999%) were annealed at 500 °C for 5 h in a vacuum of $10^{-3}$ Pa to remove the mechanical stress and obtain homogeneous structure over a large area. Anodization was carried out for 4 h with different kinds of electrolytes to form the holes with different diameters, and Table 1 lists the anodization conditions for getting well-ordered nanohole arrays. After removing the alumina layer formed at the above step in a mixture of phosphoric acid (6 wt %) and chromic acid (1.5 wt %), the aluminum foils were oxidated again at the same conditions as the first step for 12 h, and then the PAAM template was etched by saturated $SnCl_4$ solution to remove the remaining aluminum. The alumina barrier layer was then dissolved in 5 wt % $H_3PO_4$ solution at 30 °C. Finally, a layer of Au film was sputtered onto one side of the PAAM template to serve as the working electrode.

The electrolyte for Ni nanowires preparation contains a mixture of 100 g/L $NiSO_4 \cdot 6H_2O$, 30 g/L $NiCl_2 \cdot 6H_2O$, 40 g/L $H_3BO_3$ solution, and the pH value was adjusted to 2.5 with 1 M $H_2SO_4$. Ni nanowire arrays were fabricated by the direct current electrodeposition into the holes of PAAM with the potential of 1.35 V at 10 °C.

To synthesize large-area, high-filling, and single-crystal Ni nanowire arrays, attention should be paid to several factors. First,

* Corresponding author. E-mail: gtfei@issp.ac.cn; Fax: +86-551-5591434.

10.1021/jp053627i CCC: $30.25 
Published on Web 12/03/2005

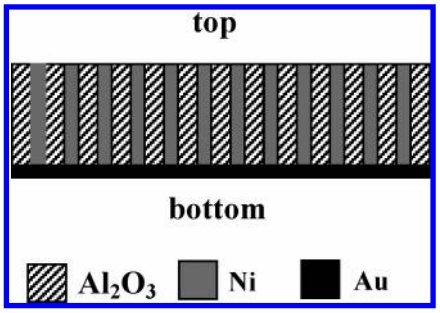


**Figure 1.** Schematic representation of the Ni nanowires in the PAAM.

the pretreatment of PAAM template is necessary, such as sonicleaning in the deionized water to drive out air inside the holes of the templates and deposit electrolyte solution into the holes of the templates. Second, the higher the potential, the faster the nucleation rate, which makes the deposited metal nanowires polycrystalline.[21,22] Meanwhile, the possibility of hydrogen gas formation will increase under a higher potential in the holes of PAAM. Small hydrogen gas bubbles will block the migrating path of metal ions in the holes, which will obstruct the growth of metal nanowires in the holes. However, Pan et al. reported that single-crystal Ni nanowires can be prepared at slightly higher potential by the direct current electrodeposition into the holes of PAAM, and thought that only at the deposition potential of above 1.0 V can the single-crystal Ni nanowires be produced.[23] We have tried this method and found that single-crystal Ni nanowires can be fabricated, but there are many gas bubbles produced during the electrodeposition process, which might influence the filling rate of Ni nanowires. In our case, Ni nanowires were prepared at the potential of 1.35 V. Third, the increase of deposition temperature at a constant deposition potential may lead to the appearance of polycrystalline nanowires because thermal energy agitates the growth and distorts the competition between adjacent grains.[18] We have prepared Ni nanowires at different temperatures and confirmed the above viewpoint. To explore the effect of size confinement on growth orientation of Ni nanowires, deposition temperature was kept at 10 °C for all samples. Finally, many papers have reported that the pH value of solution has no influence on the structure of Ni nanowires.[17,18,23] The electrodeposition at higher pH solution gives rise to the lower quality product, probably due to the appearance of a second phase usually composed of oxide or hydroxide.[24] However, if the pH value is too low, the solution will erode the PAAM template. Therefore, the pH value of the solution was adjusted to 2.5 with 1 M $H_2SO_4$ in our experiment. In all of our experiments, the pH value of electrolyte, temperature, and the potential were kept unchanged during the whole electrodeposition process. The scheme for Ni nanowires in PAAM is shown in Figure 1.

The growth orientation of Ni nanowires was characterized by X-ray diffractometer (Philips X'Pert) with Cu $K\alpha_1$ radiation ($\lambda = 0.154056$ nm). The morphologies of nanowire arrays were observed with field-emission scanning electron microscopy (FE-SEM, JEOL JSM-6700F) and high-resolution transmission electron microscopy (HRTEM, JEOL-2010). For X-ray diffraction (XRD) measurements, the overfilled nanowires on the surface of the PAAM template were mechanically polished away. For SEM observations, the PAAM was partly dissolved with 0.5 M NaOH solution, and then carefully rinsed with deionized water for several times. For TEM observations, the PAAM was completely dissolved with 1 M NaOH solution and then rinsed with absolute ethanol.

## Results and Discussion

Figure 2 shows the FE-SEM morphologies of the as-prepared PAAM templates, which were anodized under the conditions of the Table 1. From Figure 2 we can see that the average diameter of the pores in PAAM templates is about 25, 45, 90, and 225 nm, respectively. Almost perfect domains of hexagonally arranged pores can be seen in Figure 2a−c. However, the bigger holes anodized with phosphoric acid (Figure 2d) are not as ordered as those anodized in oxalic or sulfuric acids.

The top-view images of Ni nanowires electrodeposited into the holes of PAAM with the diameter of 25, 45, 90, and 225 nm, respectively, are presented in Figure 3. It can be seen that the diameter of nanowires is corresponding well to the diameter of nanoholes, and large numbers of Ni nanowires were produced in the PAAM template, where some nanowires congregated after dissolving PAAM partly.

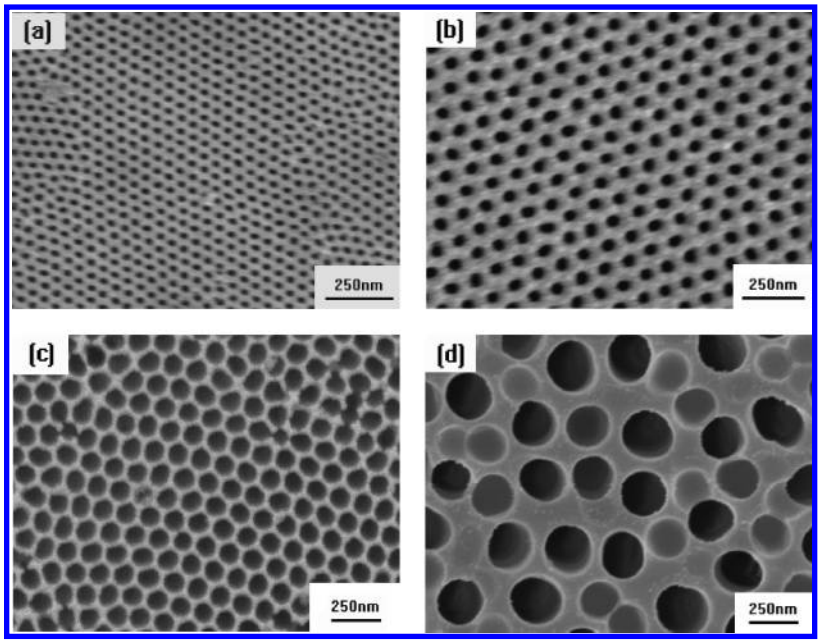


**Figure 2.** SEM top views of PAAM templates. The PAAM templates were prepared by anodized in 0.3 M sulfuric acid (a), 0.3 M oxalic acid (b), 0.3 M oxalic acid after etching in the 5 wt % phosphoric acid for about 45 min (c), 0.1 M phosphoric acid (d).

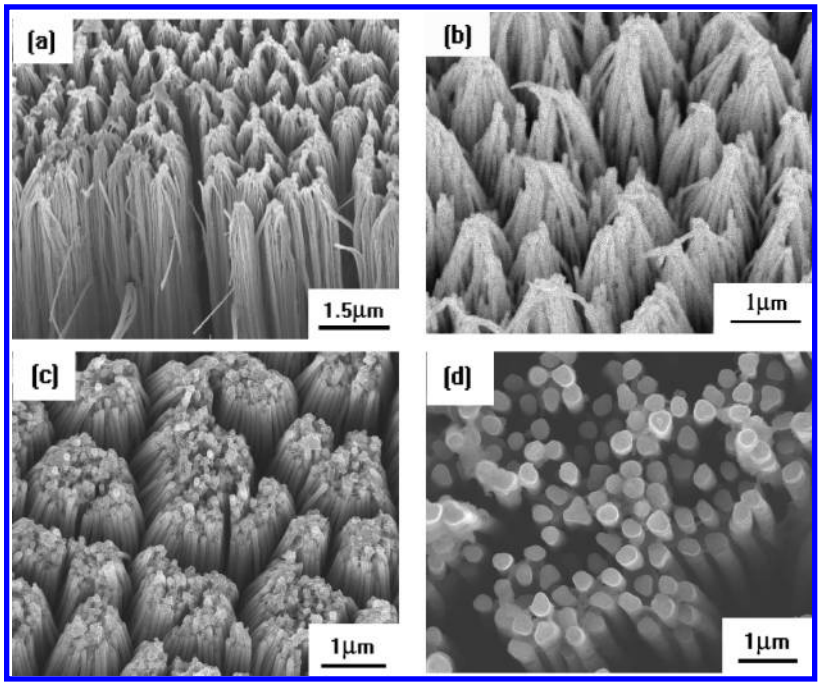


**Figure 3.** SEM photographs of Ni nanowire arrays with different diameters: (a) 25 nm, (b) 45 nm, (c) 90 nm, and (d) 225 nm.

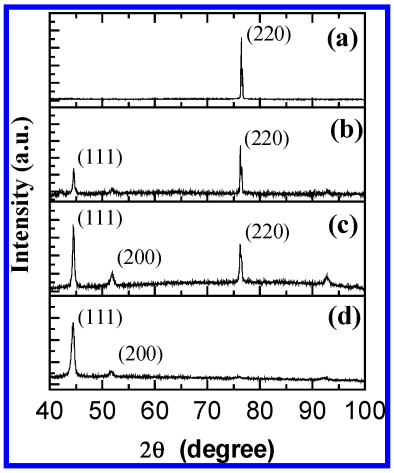


**Figure 4.** XRD patterns of Ni nanowire arrays with different diameters: (a) 25 nm, (b) 70 nm, (c) 90 nm, (d) 225 nm.

The XRD patterns of Ni nanowire arrays with different diameters are shown in Figure 4, which were collected from the top sides of Ni nanowire arrays in Figure 1. All the positions of the peaks are in good agreement with those of the face-centered cubic (FCC) Ni (JCPDS, 04-0850). It can be seen from Figure 4a that for the Ni nanowires with the diameter of 25 nm, there is only one peak of the (220) plane, which indicates that Ni nanowires have a well-preferred growth orientation along [110] direction. As for the diameter of 45 nm, the nanowires have the same growth orientation, which is not shown here. When the diameter of nanowires increases to 70 nm, two peaks of (111) and (220) planes appear, as shown in Figure 4b, which means that some nanowires grow along the [110] direction and others along the [111] direction. However, the intensity for (220) planes is much higher than that of (111) planes, indicating that most nanowires still grow along the [110] direction. With the diameter increasing to about 90 nm, the peak intensity of (111) planes is higher than that of (220) planes (Figure 4c), indicating that most nanowires grow along the [111] direction. Furthermore, when the diameter of nanowires increases to 225 nm, the Ni nanowires have a strong [111] preferred orientation (Figure 4d), which is consistent with the results of Whitney et al.[25] From Figure 4, we can see that when the diameter is small, the Ni nanowires prefer to grow along the [110] direction, whereas they will grow along the [111] direction with increasing diameter of nanowires. It seems that the growth orientation of Ni nanowires turns from [110] to [111] at the diameter between 70 and 90 nm.

It is well-known that the penetrating length of X-ray is limited to about several micrometers for Ni, so Figure 4 gives only the growth orientation of the top part of nanowires. To confirm the results that the growth orientation is formed at the beginning of nanowires growth or not, the Au film on the PAAM in Figure 1 was carefully removed partly, so X-rays can penetrate the Au film and reach the Ni nanowires. The XRD patterns obtained from the bottom side are the same as the results of Figure 4, except for the peaks of Au. This indicates that the growth orientation starts from the beginning of Ni nanowire growth.

The growth orientation was further confirmed by TEM and SAED. In Figure 5 the typical TEM images and SAED patterns of single-crystal structures of Ni nanwires with diameter of 25 and 225 nm are clearly illustrated. It can be found from Figure 5a and b that Ni nanowires with diameter of both 25 and 225 nm are long and continuous, and the diameter of the nanowires is highly uniform. The SAED patterns taken at different areas along the nanowires with diameter of 25 and 225 nm respectively do not change, which indicates that the nanowires with diameter of 25 and 225 nm are single-crystalline. From the SAED patterns in Figure 5a and b, we can see that the growth orientation is [110] and [111], respectively.

Figure 6 shows typical TEM and corresponding HRTEM images of Ni nanowires with diameter of 25 and 225 nm. The HRTEM image of Ni nanowires with diameter of 25 nm in Figure 6b clearly shows lattice fringes of (111), (002), and (220) planes, suggesting the single-crystal structure. It can be seen from Figure 6b that the [110] direction is along the axis of nanowire with diameter of 25 nm shown in Figure 6a. The HRTEM image in Figure 6d is a little dim because the diameter of nanowire is too large. However, from Figure 6d we can also see that the interplanar spacing is corresponding to the (111) plane of cubic Ni, and the growth of Ni nanowire with diameter of 225 nm is along the [111] direction.

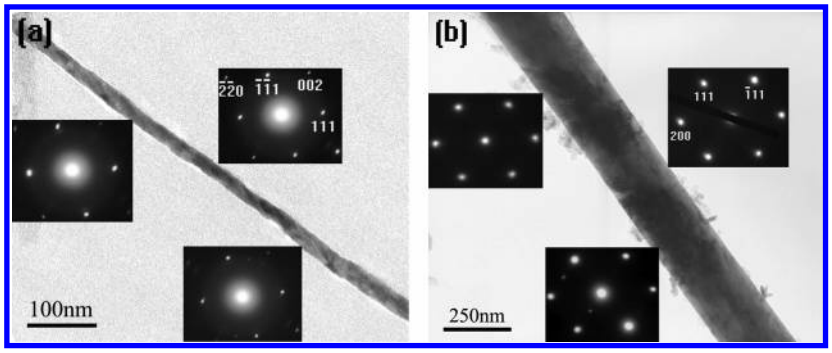


**Figure 5.** TEM images of Ni nanowires and corresponding SAED patterns taken from different areas along the nanowires: (a) diameter of 25 nm, (b) diameter of 225 nm.

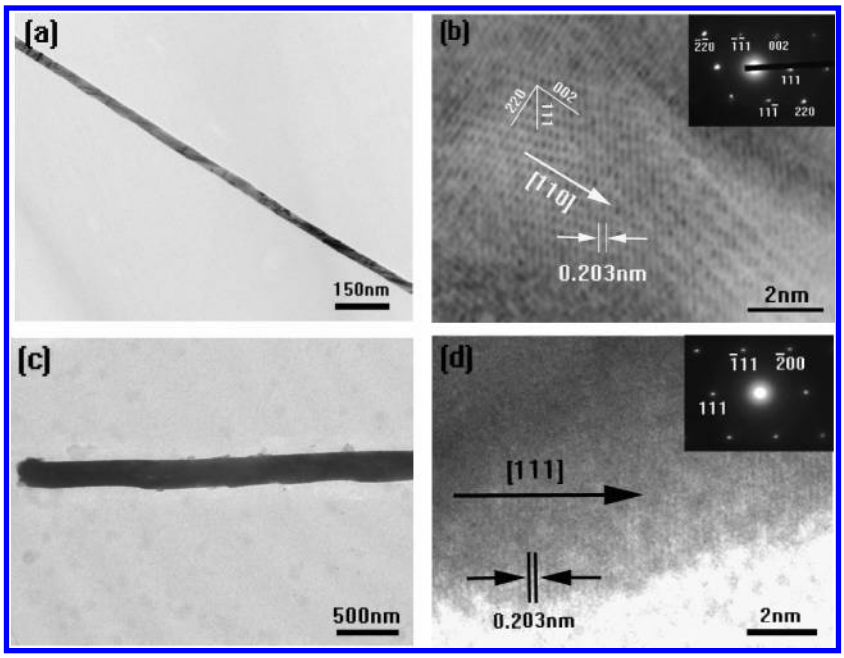


**Figure 6.** TEM and HRTEM images of Ni nanowires: (a) TEM image of Ni nanowire with diameter of 25 nm, (b) HRTEM image corresponding to the nanowire shown in (a), (c) TEM image of Ni nanowires with diameter of 225 nm, (d) HRTEM image corresponding to the nanowire shown in (c).

X-ray diffraction study was further carried out with the Ni nanowire arrays after annealing in a vacuum of $10^{-3}$ Pa at 750 °C for 4 h, and the diffraction patterns are the same as those shown in Figure 4, which suggests that the relation between growth orientation and the diameter of nanowires is intrinsic. Moreover, to know the effect of work electrode Au on the growth orientation of Ni, we elecrodeposited Ni on the Au surface. The results indicate that almost all peaks of Ni appear, which means that the Au surface has no effect on the growth orientation of Ni nanowires. Meanwhile, all samples were fabricated at the same electrodeposition conditions. So we think the diameter of PAAM has effect on the growth of Ni nanowires.

Thermodynamically, the growth of nanowires should satisfy the energy minimum principle. For the bulk metal with FCC structure, the (111) plane is a low energy plane, so [111] should be the growth direction.[26] In our experiment, there exists the following interface energy: Ni/Au, Ni/$Al_2O_3$ and Ni/electrolyte, and different plane of Ni can result in different interface energy. The area between Ni and Au is small and fixed. Moreover, our experimental results indicate that the polycrystalline Au substrate has no effect on the Ni nanowire growth. Therefore we neglect this part here.

In our experiment, the Ni nanowire can be regard as a cylinder. The circumference side of cylinder faces $Al_2O_3$, and the bottom and top sides face Au film and electrolyte, respectively. For a cylinder, the area of circumference side $S_1$ is $\pi D\Delta h$, and the area of top side $S_2$ is $\pi D^2/4$, where $\Delta h$ is the high of the nanowire and $D$ is the diameter of nanowire. Thus the ratio of the area of circumference side to the area of top side can be shown as:

$$S_1/S_2 = 4\Delta h/D$$

Based on the same $\Delta h$, the ratio of the area of circumference side to the area of top side of cylinder will gradually increase with the decreasing of the diameter of cylinder. So, we can say that the effect of holes wall of PAAM on the growth of Ni nanowires will increase gradually with decreasing the diameter of nanowires, in other words, for the nanowires of smaller diameters, the effect of holes wall is dominant. In this case, the growth of nanowires will first satisfy the demand of interface energy between Ni and $Al_2O_3$ minimum, so the apparent growth orientation is along the [110] direction. However, for the nanowires of larger diameters, at the beginning of growth, the area of circumference side of cylinder wall is not big compared with the area of the top side of cylinder, so the preferential growth direction will be determined by the interface energy of Ni/electrolyte. In this case, nanowires will grow along their preferential direction [111]. Though the area of circumference side of cylinder between Ni and $Al_2O_3$ will increase with

increasing length of nanowires, the nanowires will keep their original growth direction because of the two-dimensional nucleation layer-by-layer growth mode.[26,27]

## Conclusion

In summary, we have successfully prepared Ni nanowire arrays by the direct current electrodeposition in the holes of PAAM templates with different diameters. The growth orientation of Ni nanowires greatly depends on the diameter of PAAM templates. When the diameter is less than 70 nm the preferential orientation of Ni nanowires is along the [110] direction, whereas nanowires will grow along the [111] direction when the diameter is larger than 90 nm. The interface energy minimum principle determines the Ni nanowire growth direction. We think the ability to prepare preferential orientation of nanowires should open up new opportunities for fundamental studies and nanostructure applications.

**Acknowledgment.** The financial support from the National Natural Science Foundation (No.19974052, 50172048, 10374090 and 10274085), Ministry of Science and Technology of China (No.2005CB623603), Hundred Talent Program of Chinese Academy of Sciences and Talent Foundation of Anhui Province (2002Z020) is gratefully acknowledged.

## References and Notes

(1) Gudiksen, M. S.; Lauhon, L. J.; Wang, J.; Smith, D. C.; Lieber, C. M. *Nature* **2002**, *415*, 617.
(2) Sun, S.; Murray, C. B.; Weller, D.; Folks, L.; Moser, A. *Science* **2000**, *287*, 1989.
(3) Kin, S. W.; Kim, M.; Lee, W. Y.; Hyeon, T. *J. Am. Chem. Soc.* **2002**, *124*, 7642.
(4) Lee, S. B.; Mitchell, D. T.; Trofin, L.; Navanen, T. K.; Soderlund, H.; Martin, C. R. *Science* **2002**, *296*, 2198.
(5) Li, Y.; Meng, G. W.; Zhang, L. D.; Phillip, F. *Appl. Phys. Lett.* **2000**, *76*, 2011.
(6) Wu, Y. Y.; Yang, P. D. *Adv. Mater.* **2001**, *13*, 520.
(7) Zong, R. L.; Zhou, J.; Li, Q.; Du, B.; Li, B.; Fu, M.; Qi, X. W.; Li, L. T.; Buddhudu, S. *J. Phys. Chem. B* **2004**, *108*, 16713.
(8) Li, H.; Pederiva, F.; Wang, B. L.; Wang, J. L.; Wang, G. H. *Appl. Phys. Lett.* **2005**, *86*, 011913.
(9) Zhang, J. X.; Zhang, L. D.; Ye, C. H.; Chang, M.; Yan, Y. G.; Lu, Q. F. *Chem. Phys. Lett.* **2004**, *400*, 158.
(10) Wang, X. F.; Zhang, J.; Shi, H. Z.; Wang, Y. W.; Meng, G. W.; Peng, X. S.; Zhang, L. D. *J. Appl. Phys.* **2001**, *89*, 3847.
(11) Vazquez, M.; Pirota, K.; Hernandez-Velez, M.; Pride, V. M.; Navas, D.; Sanz, R.; Batallan, F.; Velazquez, J. *J. Appl. Phys.* **2004**, *95*, 6642.
(12) Li, C.; Zhang, D. H.; Han, S.; Liu, X. L.; Tang, T.; Zhou, C. W. *Adv. Mater.* **2003**, *15*, 143.
(13) Gudiksen, M. S.; Wang, J. F.; Lieber, C. M. *J. Phys. Chem. B* **2002**, *106*, 4036.
(14) Wang, R. P.; Xu, G.; Jin, P. *Phys. Rev. B* **2004**, *69*, 113303.
(15) Wu, Y.; Cui, Y.; Huynh, L.; Barrelet, C. J.; Bell, D. C.; Lieber, C. M. *Nano Lett.* **2004**, *4*, 433.
(16) Abel, S.; Freimuth, H.; Lehr, H.; Mensinger, H. *J. Micromech. Microeng.* **1994**, *4*, 47.
(17) Rahman, I. Z.; Razzeeb, K. M.; Rahman, M. A.; Kamruzzaman, M. *J. Magn. Magn. Mater.* **2003**, *262*, 166.
(18) Pan, H.; Liu, B. H.; Yi, J. B.; Poh, C.; Lim, S. H.; Ding, J.; Feng, Y. P.; Huan, C. H. A.; Lin, J. Y. *J. Phys. Chem. B* **2005**, *109*, 3049.
(19) Masuda, H.; Fukuda, K.; *Science* **1995**, *268*, 1466.
(20) Sander, M. S.; Gronsky, R.; Sands, T.; Stacy, A. M. *Chem. Mater.* **2003**, *15*, 335.
(21) Jin, C. G.; Jiang, G. W.; Liu, W. F.; Cai, W. L.; Yao, L. Z.; Yao, Z.; Li, X. G. *J. Mater. Chem.* **2003**, *13*, 1743.
(22) Tian, M. L.; Wang, J. G.; Kurtz, J.; Mallouk, T. E.; Chan, M. H. W. *Nano Lett.* **2003**, *3*, 919.
(23) Pan, H.; Sun, H.; Poh, C.; Feng, Y.; Lin, J. *Nanotechnology* **2005**, *16*, 1559.
(24) Holam, M.; O'Keefe, T. J. *Miner. Eng.* **2000**, *13*, 193.
(25) Whitney, T. M.; Jiang, J. S.; Searson, P. C.; Chien, C. L. *Science* **1993**, *261*, 1316.
(26) Moller, F. A.; Kintrup, J.; Lachenwitzer, A.; Magnussen, O. M.; Behm, R. J. *Phys. Rev. B* **1997**, *56*, 12506.
(27) Lachenwitzer, A.; Magnussen, O. M. *J. Phys. Chem. B* **2000**, *104*, 7424.